IEEE Access
Multidisciplinary ⋮ Rapid Review ⋮ Open Access Journal

Received 14 June 2024, accepted 4 August 2024, date of publication 9 August 2024, date of current version 20 August 2024.

Digital Object Identifier 10.1109/ACCESS.2024.3441107

RESEARCH ARTICLE

Modeling and Detailed Analysis of Rule Based, Conventional Fuzzy and Type-II Fuzzy Logic Energy Management Systems of Fuel Cell-Battery Hybrid Powered Unmanned Aerial Vehicles

ZEHRA URAL BAYRAK AND MERVE NUR KAYA
School of Aviation, Department of Avionics, Firat University, 23119 Elâzığ, Türkiye
Corresponding author: Zehra Ural Bayrak (zural@firat.edu.tr)

This work was supported by the Scientific Research Projects Coordination Unit of Firat University under Project SHY.24.02.

ABSTRACT The emissions that aircraft discharge into the atmosphere are growing daily as a result of advancements in the aviation sector and an increase in air traffic. For this reason, studies on the use of more electricity in the field of aviation have also increased. Development in battery technologies accelerates the transition to electric systems. Hybrid systems are preferred to increase the system efficiency and to ensure longer lifespan of energy sources. With this motivation, a hybrid Unmanned Aerial Vehicle (UAV) system in which Fuel Cell (FC) is the main power source and Lithium Ion (Li-ion) battery assists FC in sudden power changes is modelled and analyzed in Matlab/Simulink environment. In hybrid systems, Energy Management System (EMS) is needed to control energy resources and increase the efficiency of the UAVs. In this study, three different EMS structures in UAVs, including rule-based Thermostat on/off, classical and Type-II fuzzy logic are analyzed in detail. These EMS methods are modeled and examined for the hybrid UAV system. The unique value of this study is to apply three different EMS methods to a UAV powered by a fuel cell and Li-ion battery. An important contribution has been made to researchers that the preferred EMS method may be different depending on the system to be used and the number of resources. Although Type-II fuzzy logic EMS gives better results, it is more complex and the decision-making time is longer. For this reason, traditional fuzzy logic EMS is more widely used in most applications.

INDEX TERMS Fuel cell, UAV, EMS, rule based, type II fuzzy logic.

NOMENCLATURE

E_n	:Nernst voltage (V).
F	:Faraday constant (96485 A s/mol).
h	:Planck's constant (6.626×10^{-34} J s).
I_{nom}	:Nominal current (A).
k	:Boltzmann's constant (1.38×10^{-23} J/K).
K	:Voltage undershoot constant.
K_c	:Voltage constant at nominal condition of operation.
N	:Number of cells.
P_{air}	:Absolute supply pressure of air (atm).
P_{airnom}	:Nominal absolute air supply pressure (Pa).
P_{fuel}	:Absolute supply pressure of fuel (atm).
P_{H2}	:Partial pressure of hydrogen inside the stack (Pa).
P_{H2O}	:Partial pressure of water vapor inside the stack (atm).
P_{O2}	:Partial pressure of oxygen inside the stack (Pa).
R	:Universal gas constant (8.3145 J/mol K).
T	:Temperature of operation (K).

The associate editor coordinating the review of this manuscript and approving it for publication was Wojciech Sałabun.

T_{nom}	:Nominal operating temperature (K).
w	:Percentage of water vapor in the oxidant (%).
x	:Percentage of hydrogen in the fuel (%).
y	:Percentage of oxygen in the oxidant (%).
z	:Number of moving electrons.
$V_{lpm(air)}$	:Air flow rate (l/min).
$V_{lpm(air)nom}$	:Nominal air flow rate (l/min).
$V_{lpm(fuel)}$	:Fuel flow rate (l/min).
V_{nom}	:Nominal voltage (V).
Greek Symbols	
α	:Charge transfer coefficient.
ΔG	:Size of the activation barrier (J/mol).
$\Delta h_0(H_2O(gas))$	:241.83 × 103 J/mol.
Δv	:Activation barrier volume factor (m^3).
η_{nom}	:Nominal LHV efficiency of the stack (%).

I. INTRODUCTION

Recently, the use of electrical systems in Unmanned Aerial Vehicles (UAVs) has become widespread due to their higher efficiency, lower greenhouse gas emissions and less noise features. The electrical energy required by UAVs is generally provided by batteries. However, the goals set by the European Union by 2050 include reducing net greenhouse gas emissions to zero and ensuring economic and social sustainability. Fuel cells (FCs) have a high energy density, low noise and emission characteristics that make them the cleanest alternative energy source for transportation [1], [2].

FCs are electrochemical devices that use the chemical energy in hydrogen to generate electricity. The FC consists of two electrodes, a catalyst to quicken the chemical reaction, and an electrolyte to transfer electrically charged particles between electrodes [1], [3]. Protons pass by the electrolyte membrane while electrons create current in the FC when hydrogen molecules break into electrons and protons [4]. These protons, electrons, and oxygen unite to form water molecules at the cathode. Water vapor is produced as a result, which distinguishes FCs from other options in terms of emission targets [5], [6].

Depending on their working temperatures, efficiency, applications, and costs, FCs are employed in a variety of applications. Depending on the kind of fuel and electrolyte used in FCs, they are grouped together [7]. FC types can be listed as Proton exchange membrane (PEM) FC, Alkaline FC, Phosphoric Acid FC, Molten Carbonate FC, Solid Oxide FC, Direct methanol FC. Among different FC types, PEMFC is preferred in this study because it has high efficiency and power density, requires lower operating temperatures and responds quickly to loading [8].

A battery is a type of portable energy storage that consists of several electrochemical cells that may store electrical energy as chemical energy. The most suitable battery type used in UAVs is adjusted by bench marking the power density, energy density, weight, volume, cycle life, cost, safety and maintenance features of the batteries [9].

When choosing a battery, the characteristics of the cells, serial or parallel connections, the number of cells used and the external hardware structure are taken into consideration [10]. Connecting battery packs in series allows for higher voltage. This allows high power to be obtained even with lower current. Higher power contributes to better performance of the vehicle, especially in electric vehicles. High voltage can enable more effective energy transfer and lower energy losses [11]. Lithium-Ion (Li-ion) batteries have advantages such a lower self-discharge rate when not in use and an energy-to-weight ratio when compared to other battery technologies. In addition, they are more widely preferred in UAVs because they cause less harm to the environment compared to other battery types [12].

Li-ion batteries have a lightweight structure. Each cell has an output voltage of approximately 4 V and an energy level of 100-150 Wh/kg. These batteries have a cycle life of 2000 and can operate at temperatures between −20°C and +60°C [13], [14], [15].

Batteries used to store energy need time to recharge as their charge decreases as they are used [1]. Fast charging models are used to reduce this required time and the cycles of batteries [1], [16]. Hybrid systems are preferred to solve this problem and increase efficiency in UAVs. FC hybrid systems are used in different application areas such as aviation, automotive or railway [17], [18], [19], [20].

In hybrid systems, Energy Management System (EMS) is needed to determine the operating range of the power supplies and ensure accurate operation of the system. EMS coordinates the system operation and uses a control algorithm to optimize the system by taking into account time-based conditions [21]. EMSs are basically classified as Rule based, optimization based and learning based [22], [23]. In the hybrid system proposed in this study, rule-based EMS and conventional fuzzy logic EMS methods are used and the results are compared with each other.

Brushless Direct Current (BLDC) motor is preferred as the motor type for the UAV proposed in this study. Various types of UAVs, including quadcopter, octocopter, tricopter, duocopter, and helicopter, use brushless motors with different features. Because of its straightforward design, extended lifespan, low maintenance requirements, and great power, this engine type is utilized in UAVs [24]. Advancements in technology have made it possible to create BLDC at high speeds. UAVs can now be used in more regions because to these advancements. They are employed in a variety of industries, including commercial aerial photography, freight transportation, military reconnaissance, and meteorological observation [24], [25], [26].

There are studies in the literature where hybrid systems are used in electric vehicles. For this reason, EMS was also needed. A detailed review of similar studies that will guide this study is given below.

Lu et al. [27] discussed an approach to optimally solve EMS in hybrid electric vehicles with FCs. This study highlights the significant influence that the degree of battery degradation plays for EMS as an internal component.

Şefkat and Özel [28] used a fuzzy logic controller to increase the energy efficiency of a FC hybrid electric vehicle. It contains a thorough mathematical model intended to keep the battery and hydrogen fuel cell operating at their ideal temperatures.

Zhang et al. [29] is examined in terms of the hybrid power system of a city train in order to reduct the total cost by optimizing component sizes. Three alternative optimization techniques were used to optimize the system in order to compare how well the suggested strategy performed.

Xiu et al. [30] examined the hybrid use of a hydrogen FC and battery in submarine vehicles. They proposed the use of FCs to increase the durability of unmanned submarine vehicles.

In a study by Tao et al. [31], hybrid electric vehicles supported by FCs, batteries and supercapacitors were discussed. The complex structures of these vehicles, variable terrain conditions and the difficulties they create in terms of energy management, lifespan of power supplies and fuel economy have been examined. An EMS containing path information obtained by a deep learning algorithm is proposed.

In a study by Shen et al. [32], a hybrid system consisting of FC, battery and supercapacitor was examined for electrical vehicles. To create the hybrid power system, a variable structure battery plan is suggested. To guarantee that the FC runs at maximum efficiency and generates an incremental power output within the permitted power gradient, a fuzzy logic EMS was developed.

Ghavidel and Mousavi [33] examined at stable control techniques and dynamic modeling analysis for hybrid energy systems that included a supercapacitor, battery, and FC. The suggested plan seeks to prevent abrupt shifts in the power supplies' dynamic response. An EMS fuzzy algorithm for hybrid energy storage systems is presented. Performance and efficiency analyze of this hybrid system were examined for a tramway.

The study by Liu et al. [34] discusses EMS, which was developed to solve complex energy management problems and optimize economy and performance of hybrid vehicles containing FCs, batteries, and supercapacitors.

The study by Rodriguez et al. [35] focused on the EMS of hybrid electric vehicles with FCs. A modular EMS has been proposed for a dual-mode locomotive hybrid electric vehicle.

The hybrid systems in the literature examined in detail above are designed for applications of electric vehicle. However, in this study, the hybrid system is proposed for UAV application. The methods used to increase the energy efficiency of hybrid electric vehicles in the literature will be applied to the UAV. Information about studies on EMS methods used in UAVs is given below.

Cheng et al. [36] discussed the issue that the low durability of battery-powered UAVs can be improved by applying a hybrid system with a FC, and that energy management can greatly affect the performance of this hybrid system. They provided energy control by proposing four different EMS. Proposed EMSs are fuzzy logic, dynamic programming, Pontryagin's minimum principle and improved Pontryagin's minimum principle.

A genetic algorithm based optimized rule based EMS for the best possible power distribution between the FC and battery system is suggested in the study conducted by Yuan et al. [37]. Battery charging sustainability is the aim of control variables in real time rule based EMS, taking FC efficiency and durability into account.

The study by Xiao et al. [38] concentrated on hybrid power systems consisting of PEMFC and lithium batteries, which are generally recommended to increase the flight times of high-performance UAVs. In order to regulate the PEMFC, the suggested design places an automatic on/off switch in parallel with a DC-DC converter. To control the lithium battery, a second automatic on/off switch takes the place of the conventional DC-DC converter.

Townsend et al.'s study [39] looked at a hybrid system that included a supercapacitor, battery, and FC. Reducing hydrogen consumption and extending the life of the resources were the goals of the EMS. It has been suggested to create a new EMS based on a modified proportional-integral controller that takes FC efficiency into account.

Oksuztepe et al. [40] examined the behavior of a fixed-wing PEMFC/Supercapacitor hybrid UAV. The study investigates the performance of this aircraft at different flight levels. They stated that flight levels negatively affected PEMFC. They validated the proposed UAV model in MATLAB/Simulink.

Unlike the EMS systems suggested in the literature, three different EMS methods are examined in detail in this paper. This study's goal is to increase the efficiency of hybrid UAVs by extending the battery life and to ensure more active use of resources. For this purpose, the outputs of the battery and FC operating under specified conditions are examined to increase the range and efficiency of hybrid electric UAVs. The operating ranges of the battery and FC are determined under the desired conditions according to temperature, altitude and the SoC of the battery. First of all, the thermostat (on/off) strategy deterministic is examined within the rule-based EMS, which determines the operating status of the source as on/off according to the created conditions. Then, conventional fuzzy logic and type-II fuzzy logic, which are among the rule-based EMSs that can express more situations under the same conditions, are examined. Finally, the rule-based EMS types used in the study are compared with each other. Using rule-based EMS in a hybrid UAV application and analyzing it in detail will help scientists working on this subject.

II. HYBRID UAV SYSTEM POWERED BY FUEL CELL AND BATTERY

When FCs are used as a power source in UAVs, they may not respond quickly to instantaneous current changes. For this reason, using it as a hybrid with a secondary source having high power density will increase the efficiency of the system. Li-ion batteries, on the other hand, may not provide sufficient flight time in UAVs by the reason of their low energy density and long charging times. A hybrid system design that eliminates the disadvantages of both sources is the best solution for UAVs [23].

A. PEM FUEL CELL

With its outstanding qualities including high efficiency, non-pollution, and quick charging, FC technology—a developing energy production device—can meet the energy demands of a variety of industries, including transportation, aviation, and maritime [41].

PEMFCs are the most widely used FC type [42]. The catalyst causes the hydrogen in the anode to break down into protons and electrons [43]. While electrons must pass via an external circuit to reach the cathode, protons can pass through the membrane directly. Moreover, water is produced as waste when protons and oxygen in the cathode react. Electrochemical processes proceed and a continuous current is produced as long as hydrogen is available [3]. PEMFCs typically function in the 65–85 °C range, and because of the water produced on the cathode side, the PEMFC must operate below 100 °C [44].

Chemical reactions occurring in PEMFC are given in Eq.1-3 [45]:

$$\text{Anode reaction:} \quad 2H_2 \rightarrow 4H^+ + 4e \tag{1}$$

$$\text{Cathode reaction:} \quad O_2 + 4H^+ + 4e \rightarrow 2H_2O \tag{2}$$

$$\text{Overall reaction:} \quad 2H_2 + O_2 \rightarrow 2H_2O \tag{3}$$

PEMFCs need to be modeled in order to perform detailed simulations. The polarization curve of a particular PEMFC working under optimum temperature and pressure specifications consists of three regions: activation, ohmic and mass transport. The activation voltage drop brought on by the sluggishness of the chemical reactions taking place on the electrode surfaces is represented by the activation area. The type of electrode and catalyst utilized, the operating pressure and temperature, all affect this region.

The resistance losses brought on by the PEMFC stack's internal resistance are represented by the ohmic region. Lastly, when the fuel is utilized, the mass transport area depicts the mass transport losses brought on by the shift in reactance concentration [46].

Open circuit voltage (E_{OC}), current (i_0), and Tafel slope (A) will all fluctuate in response to changes in variables like pressure, temperature, fuel and air composition, and flow rates. These changes are given in Eq. 4-6.

$$E_{OC} = K_C E_n \tag{4}$$

$$i_0 = \frac{zFk(P_{H_2} + P_{O_2})\Delta v}{Rh} e^{\frac{-\Delta G}{RT}} \tag{5}$$

$$A = \frac{RT}{z\alpha F} \tag{6}$$

The equivalent circuit of detailed model is the same as the simplified model in Matlab/Simulink, but the parameters E_{OC}, i_0, and A need to be updated. The usage rates of hydrogen (U_{fH_2}) and oxygen (U_{fO_2}) are given in Eq 7 and 8.

$$U_{fH_2} = \frac{n^r_{H_2}}{n^{in}_{H_2}} = \frac{60000RTNi_{fc}}{zFP_{fuel}V_{lpm(fuel)}x\%} \tag{7}$$

$$U_{fO_2} = \frac{n^r_{O_2}}{n^{in}_{O_2}} = \frac{60000RTNi_{fc}}{zFP_{air}V_{lpm(fuel)}y\%} \tag{8}$$

Partial pressures and Nernst voltage are calculated as Eq 9-12.

$$P_{H_2} = \left(1 - U_{f_{H_2}}\right) x\%P_{fuel} \tag{9}$$

$$P_{H_20} = \left(1 - 2y\%U_{f_{O_2}}\right) x\%P_{air} \tag{10}$$

$$P_{H_20} = \left(1 - U_{f_{O_2}}\right) y\%P_{air} \tag{11}$$

$$E_n = \begin{cases} 1.229 + (T - 298)\dfrac{-44.43}{zF} + \dfrac{RT}{zF}\ln(P_{H_2}P_{O_2}^{1/2}), \\ \qquad T \leq 100°C \\ 1.229 + (T - 298)\dfrac{-44.43}{zF} + \dfrac{RT}{zF}\ln\left(\dfrac{P_{H_2}P_{O_2}^{1/2}}{P_{H_2O}}\right), \\ \qquad T \geq 100°C \end{cases} \tag{12}$$

Nominal conversion rates of gases are calculated by Eq. 13 and 14.

$$U_{f_{H_2}} = \frac{\eta_{nom}\Delta h^0\,(H_2O\,(gas))\,N}{zFV_{nom}} \tag{13}$$

$$U_{f_{O_2}} = \frac{60000RT_{nom}NI_{nom}}{2zFP_{air_{nom}}V_{lpm(air)_{nom}} * 0.21} \tag{14}$$

The nominal partial pressures and Nernst voltage of the gases can be determined from these conversion rates. α, ΔG, and K_C can be found if E_{OC}, i_0, and A are known and the stack functions at constant utilization rates under nominal conditions. The highest possible fuel and air flow rates set a limit on the maximum current a PEMFC can deliver. As more current is drawn above this maximum amount, the voltage output of the stack abruptly decreases. Oxygen depletion (caused by air compressor delay) is modeled in terms of peak consumption ($U_{f_{O_2}}$peak) and the corresponding drop below voltage goal. As a result, the Nernst voltage is altered as per Eq. 15:

$$E_n = \begin{cases} E_n - K(U_{f_{O_2}} - U_{f_{O_2(nom)}}), & U_{f_{O_2}} > U_{f_{O_2(nom)}} \\ E_n, & U_{f_{O_2}} \leq U_{f_{O_2(nom)}} \end{cases} \tag{15}$$

K is determined as Eq.16 [46]:

$$K = \frac{V_u}{K_c(U_{fO_2(peak)} - U_{fO_2(nom)})} \tag{16}$$

The Matlab/Simulink model whose equations are given above is used in this study. The selected PEMFC parameters are placed in Table 1.

TABLE 1. Parameters of the PEMFC.

Parameter	Value
Voltage at 0A and 1A	42 V - 35V
Nominal operating point	52 A - 24.23 V
Maximum operating point	100 A – 20 V
Number of cells	42
Nominal stack efficiency (%)	46
Operating temperature	55 Celsius
Nominal Air flow rate	2400 lpm
Nominal supply pressure	1 - 1.5 bar
Nominal composition (%)	99.95 (H_2), 21 (O_2), 1 (H_2O air)

B. Li-ion BATTERY

The fact that batteries have different electrode and electrolyte structures diversify their usage areas. Each battery type may be better suited to certain applications and should be selected considering factors such as design preferences, cost, environmental impacts, and energy requirements [47]. Among battery types, Li-ion batteries are the most commonly used battery type due to their superiority over other battery technologies.

Information about the changes in ten features of some battery types is given in Table 2. The cycle life and power density of the Li-ion battery type are high as viewed from the table. Also, the energy efficiency is stated as 80%, which indicates the rate at which energy is kept available by the battery. The very low self-discharge rate reduces the possibility of losing energy when the battery is put on standby. Very low thermal stability means that the battery can operate safely over a wide temperature range. Low maintenance rate and no memory effect means that the battery is easier and smoother to use and maintain. The Li-ion batteries are preferred in this study because of their features such as.

Determining the remaining energy in battery usage not only improves the user experience but also ensures a long-lasting use by maintaining the health of the battery. The SoC, which expresses the ratio of this remaining energy to the rated capacity, can be found as a percentage in Eq. 17 [48].

$$SoC = \frac{Remaining\ capacity}{Rated\ Capacity} \tag{17}$$

SoC estimation for battery management systems and charge control is a challenging task due to parametric uncertainties and complexity. Coulomb counting and ampere-hour (Ah) methods are based on standardized measurement, but their reliability can be limited as they do not fully consider intrinsic and extrinsic factors. Open circuit protection and impedance measurement methods provide more reliable estimates by better reflecting the characteristics of the battery. Machine-based methods, as well as artificial neural networks and predictive logic, offer a flexible approach to parametric uncertainties and can make more effective SoC estimates by considering variable conditions such as non-consumptive use. The use of these methods requires the selection of an optimal solution depending on the characteristics of the battery and the application scenario. In this way, important objectives such as battery protection, prevention of over-discharge and battery life extension can be supplied [49].

Irreversible chemical reactions occurring in the interactions between battery active materials and the electrode cause a decrease in battery performance. This causes the battery to deteriorate over time and its internal resistance to increase. Increasing internal resistance may cause energy transfer to become more difficult and increase the battery's tendency to heat up. Increasing internal resistance and decreasing capacity indicate that the health of the battery is decreasing. State of Health (SoH) is used to evaluate and express this state. SoH indicates the battery's remaining lifespan and extent of wear. SoH refers to the ratio of the usable capacity to the nominal capacity. This shows how effective the battery is relative to its initial performance. A SoH value falling below the rated capacity indicates that the battery has aged and its original performance has been significantly reduced. Equation 19 is used to calculate the ratio of available capacity to rated capacity. This calculation is intended to determine the actual SoH of the battery and use it as a type of performance indicator. Such evaluations are important for estimating battery life, developing maintenance strategies, and monitoring battery health in energy storage systems [47], [48], [49].

$$SoH = \frac{Available\ Capacity}{Rated\ Capacity} \tag{18}$$

Systems known as electrochemical cells use redox processes to transform chemical energy into electrical energy. Li-ions are moved from the anode electrode to the cathode electrode during this process, which makes charging and discharging possible. To prevent short circuits between electrodes, a separator plate placed in the middle of the electrolyte is used. Since electron transfer is not possible through the electrolyte due to the presence of the separator plate, it occurs through an external circuit. During charging, Li-ions are transferred to the cathode electrode through the electrolyte, as they have the lowest weight and highest potential among metals. This process represents the movement of Li-ions and the operating principles of the electrochemical cell. The chemical reactions occurring in the mentioned process are important factors that determine the health status and performance of Li-ion batteries. Figure 1 shows the direction of movement of Li-ions during the charging and discharging process. The chemical reactions take placing in the mentioned process are given in Eq. 19-21 [50], [51], [52].

$$\text{Cathode Reaction; } Li_{1-x}CoO_2 + xLi^+ + xe^- \leftrightarrow LiCoO_2 \tag{19}$$

TABLE 2. Types and features of the batteries [47].

Battery Types/Features	Pb- Acid	Ni-Cd	NiMH	Zebra	Li-Po	Li-Air	Li-S	Li-ion	Zn-Br
Nominal Voltage (V)	2	1.2	1.2	2.6	3.7	2.9	2.5	3.6	1.67
Energy Density	35	50-80	70-95	90-120	130-225	1300-2000	350-650	118-250	35-54
Cycle Life	1000	2000	<3000	>1200	<1200	100	300	2000	>2000
Memory Effect	None		Rare	None	None	None	None	None	-
Operating Temperature Range (°C)	-15/+50	-20/+50	-20/+60	-240/+350	-20/60	-10/+70	-60/+60	-20/+60	-20/+60
Energy Efficiency	70	60-90	75	-	-	-	-	80	80
Overload Tolerance	High	Middle	Low	-	-	-	-	Very low	Low
Self-Discharge	Low	Middle	High	-	-	-	-	Very low	Low
Thermal Stability	Less Stable	Less Stable	Less Stable	-	-	-	-	Very low	Less Stable
Power Density	180	150	250/1000	-	-	-	-	1800	-

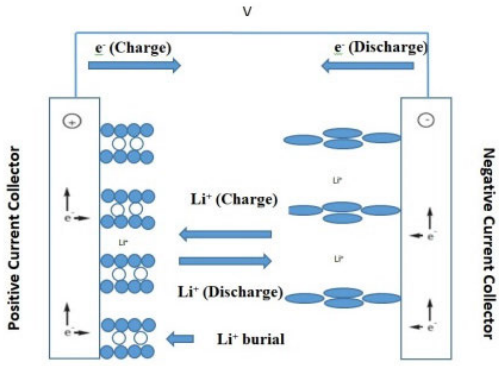

FIGURE 1. Movement direction of lithium ions.

TABLE 3. Features of the Li-ion battery used.

Parameter	Value
Nominal Voltage (V)	48
Rated Capacity (Ah)	5.4
Initial State of Charge (%)	50
Battery Response Time (s)	1
Maximum Capacity (Ah)	5.4
Cut-Off Voltage (V)	36
Fully Charged Voltage (V)	55.8714
Nominal Discharge Current (A)	2.3478
Internal Resistance (Ohm)	0.088889
Capacity (Ah) at nominal voltage	4.8835

$$\text{Anode Reaction; } CLi_x \leftrightarrow C + xLi^+ + xe^- \tag{20}$$

$$\text{Overall Reaction; } Li_{1-x}CoO_2 + CLi_x \leftrightarrow LiCoO_2 + C \tag{21}$$

Li-ion batteries, which are less harmful to the environment than other batteries, also have disadvantages such as the aging problem due to the decrease in capacity after a certain period of time, regardless of whether they are used or not, and their sensitivity to impact [15].

High power and energy per unit mass of battery can be obtained from Li-ion batteries. In addition, they are favored over other rechargeable batteries due to their reduced weight and smaller size [11]. Table 3 displays the features of the battery that was employed in this investigation.

III. ENERGY MANAGEMENT SYSTEM

The fundament of hybrid energy systems' effective operation is energy management. Although there are studies in the literature on the energy management issues with hybrid electric cars, there aren't many on the EMS techniques used with hybrid electric UAVs. Rule-based, optimization-based, and learning-based solutions are the three primary categories of energy management strategies [53]. Figure 2 makes the classification of EMS [22], [23].

Real-time power distribution can be accomplished with rule-based procedures, although the outcome is typically subpar. Rule-based solutions are commonly employed, and these tactics rely on fuzzy logic control and state machine power monitoring. Because UAVs rely too heavily on engineering skills, they are challenging to apply to long-duration,

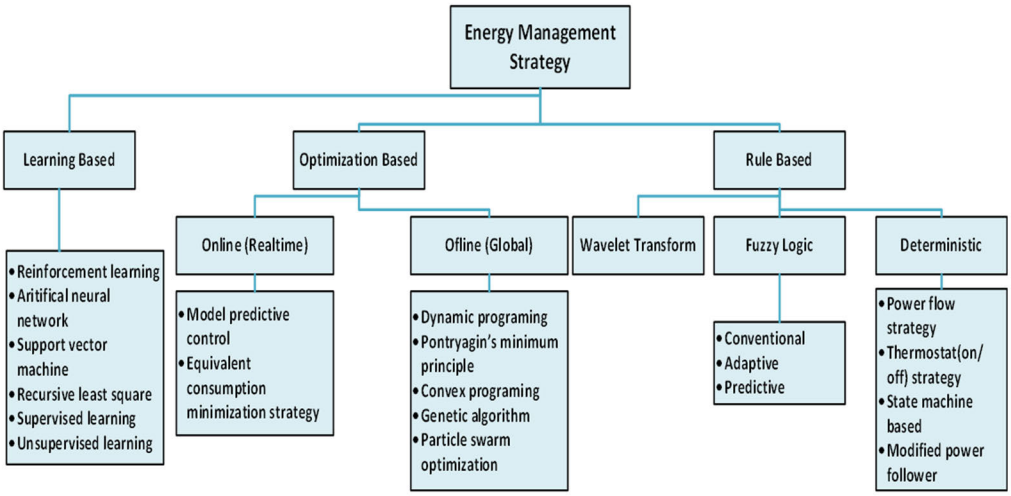

FIGURE 2. Types of EMS.

high-energy-efficiency flights. Typically, energy management problems are modeled as optimization problems by optimization-based strategies in order to increase the optimality of power allocation. These models are then solved using appropriate optimization techniques [54].

Fuzzy logic control is more resilient to system uncertainties than deterministic rule-based control because it can tolerate imprecise measurements and changes [55].

When the differences between fuzzy logic control and Type II fuzzy logic control are examined, significant differences are seen in terms of basic definitions, membership functions, uncertainty management, calculation and complexity, and application areas. In Type I fuzzy logic control, membership functions are defined with a single degree of accuracy and are usually expressed in simple shapes such as triangle, trapezoid or Gauss. Calculations of Type I systems are simpler and faster, therefore they are suitable for real-time applications and require less computational power. They are widely used in areas where uncertainty is low and fast calculations are required, such as industrial control systems, automotive and electronic devices.

Type II fuzzy logic control is an extension of Type I systems and has been developed to manage uncertainties in more detail. In Type II systems, membership functions contain uncertainty and are defined with a certain range. This range consists of two boundaries as ''lower membership function'' and ''upper membership function''. This situation represents a wider uncertainty range. Type II membership functions express the uncertainties of variables in a more flexible and complex way. However, in addition to these advantages, Type II systems require more computational power and complexity. This situation creates difficulties in real-time applications. Type II fuzzy logic control is preferred in situations where more complex and uncertain systems must be managed, such as robotics, biomedical engineering, and financial modeling [56], [57].

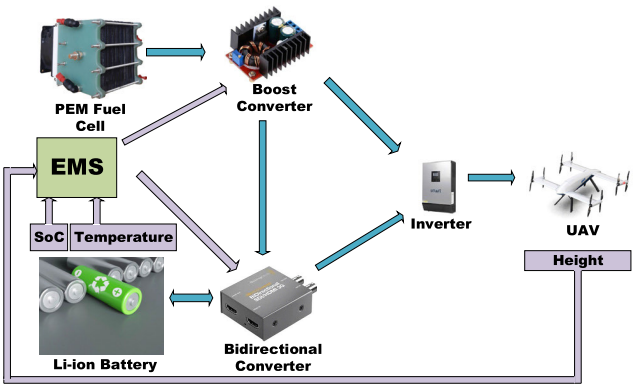

FIGURE 3. Block diagram of the UAV system.

IV. RESULTS AND DISCUSSION

The performance of a PEMFC can be described by the current-voltage characteristic. The current generated through PEMFC is proportional to the hydrogen consumption. The electrical power generated per unit of hydrogen falls as the PEMFC's voltage drops. Thus, the PEMFC voltage should be considered as a measure of the efficiency [58].

Figure 3 shows a block diagram of the suggested UAV system. In industrial applications, a boost type DC-DC converter circuit is used to raise the output voltage because PEMFCs produce low output voltage values [59]. The types of converters have a big impact on the system's efficiency. For renewable energy sources, DC-DC boost converters come in a variety of forms, including isolated double active bridge converters, full bridge converters, and resonance type boost converters, etc. [60]. They serve the purpose of raising the voltage that comes from an energy source. A boost converter is selected because the goal of this study is to raise the PEMFC's output voltage [61], [62].

The bidirectional converter is also preferred because it allows power transfer in both directions between two

dc sources. DC uninterruptible power supplies are increasingly used in applications such as battery charging circuits, telecom power supplies and computer power, as they can reverse the flow direction of current and therefore power and maintain the polarity of the voltage at both ends without changing [63].

In systems where multiple energy sources are used together, these converters provide the flexibility to switch between different voltage levels. This increases the reliability and performance of the systems. The bidirectional DC-DC converters optimize energy consumption by ensuring the efficient operation of battery systems, increase the flexibility of the systems and improve their overall performance. With these features, they play an important role, especially in areas such as renewable energy and electric transportation [64].

The inverter block contains a three-phase power converter consisting of up to six power switches connected in a bridge manner. The power switch type and converter structure are selected from the dialog box. It enabled us to convert DC to AC [65].

The flight altitude of the UAV used as a payload in this study is a factor affecting efficiency. The decrease in air density at high altitudes changes engine efficiency and aerodynamic performance, so altitude ranges ranging from 1000 to 5000 meters are used in the simulation. The wingspan and length determine the lift force and flight attitude of the UAV. While wider wings provide more lift, they also increase weight.

Flight speed directly affects the power output and energy consumption of the fuel cell. The energy management system of the UAV is optimized by considering the optimum speed and maximum speed. The optimum speed can vary between 40-100 km/h, and this speed range ensures efficient operation of the fuel cell.

Fuel cell parameters also play a critical role in determining power requirements [66]. The power output provided by the fuel cell and battery must be sufficient to operate the BLDC motors and electrical systems used in the UAV, and usually ranges from a few hundred watts to a few kilowatts. The output voltage requires that the electrical voltage provided by the fuel cell be compatible with the UAV's electrical systems and can typically be between 30-100 V. Environmental conditions also affect the performance of a fuel cell UAV. The operational temperature range can directly affect the efficiency and reliability of the fuel cell, as extreme heat or cold can reduce performance. Wind speeds and weather conditions can affect flight status and energy consumption, so aerodynamic design and a powerful energy management system ensure efficient operation of the UAV in variable environmental conditions [67].

In this article, the fixed-wing UAV model used in the author's previous study [40] is taken as reference.

In this study, a hybrid UAV system including of PEMFC and Li-ion battery is analyzed for different EMS methods. Rule based on/off thermostat EMS are examined as Case 1, conventional fuzzy logic EMS as Case 2, and Type-II fuzzy logic EMS as Case 3. The results of three different cases examined are given under subheadings.

A. CASE 1 (RULE BASED EMS)

The purpose of the designed rule-based EMS is to meet the power required by the load and control the source, taking into account the SoC and the temperature of the battery and the altitude of the UAV. In this way, the power required for the movement of the UAV will be met and resource control will be provided. The conditions considered and the desired situations are given in Table 4.

TABLE 4. Conditions of case 1.

Conditions	Conclusion
If h (altitude) is greater than 1000 m	FC enabled, battery disabled
If h (height) is less than 1000 m	FC disabled, battery enabled
If the battery temperature is greater than 45°C	FC enabled, battery disabled
If the battery temperature is less than 45°C	FC disabled, battery enabled
If SoC value is below 20%	FC enabled, battery disabled
If the SoC value is above 20%	FC disabled, battery enabled

The state variables taken into account when designing the EMS are given in Figure 4. Under normal conditions, the temperature value of the battery increases depending on the operation of the battery. However, since the simulation could not be run for a long time, the height (h) in Figure 4-a and the T temperature values in Figure 4-b are entered as constants before the simulation in order to check whether the system is working or not. The SoC value in Figure 4-c shows the current SoC status of the battery. In order to observe the rules given in the table, the SoC value of the battery is determined as 50%. As seen in Figure 4-c, the SoC value remained constant because the PEMFC is active between seconds 1-2 and 3-5.

The hybrid UAV system diagram of the rule-based EMS determined as the Case 1 is shown in Figure 5.

Simulation results of current, voltage and power curves of the battery and fuel cell, electromagnetic torque, rotor speed and load power are given in Figure 6.

It can be seen from Figure 6-a that when the battery current is zero, the battery is disabled and in these cases the FC must be activated. In Figure 6, the current of the DC/DC converter connected to the fuel cell output is given to clearly observe the moments when the battery and fuel cell are active. In Figure 6-d, when the battery is active, the current values of the FC are zero, and when the battery is not active, the system meets its needs from the FC.

As seen from Figure 6-b, although the voltage level is required to be constant at 100 V when the battery is active, it operates at approximately 50 V for a certain period of time and then reaches 100 V. When it is not activated, it exceeds 100 V. In Figure 6-e, when the FC is active, the voltage level

TABLE 5. Determined rules.

Situation	SoC	Temperature	Height	Out	Situation	SoC	Temperature	Height	Out
1	Very low	Very cold	Low	V_{fc}	**21**	Middle	Cold	Low	V_b
2	Very low	Very cold	High	V_{fc}	**22**	Middle	Cold	High	V_{fc}
3	Very low	Middle	Low	V_{fc}	**23**	Middle	Hot	Low	V_{fc}
4	Very low	Middle	High	V_{fc}	**24**	Middle	Hot	High	V_{fc}
5	Very low	Cold	Low	V_{fc}	**25**	High	Very cold	Low	V_{fc}
6	Very low	Cold	High	V_{fc}	**26**	High	Very cold	High	V_{fc}
7	Very low	Hot	Low	V_{fc}	**27**	High	Middle	Low	V_b
8	Very low	Hot	High	V_{fc}	**28**	High	Middle	High	V_{fc}
9	Low	Very cold	Low	V_{fc}	**29**	High	Cold	Low	V_b
10	Low	Very cold	High	V_{fc}	**30**	High	Cold	High	V_{fc}
11	Low	Middle	Low	V_{fc}	**31**	High	Hot	Low	V_{fc}
12	Low	Middle	High	V_{fc}	**32**	High	Hot	High	V_{fc}
13	Low	Cold	Low	V_{fc}	**33**	Very high	Very cold	Low	V_{fc}
14	Low	Cold	High	V_{fc}	**34**	Very high	Very cold	High	V_{fc}
15	Low	Hot	Low	V_{fc}	**35**	Very high	Middle	Low	V_b
16	Low	Hot	High	V_{fc}	**36**	Very high	Middle	High	V_{fc}
17	Middle	Very cold	Low	V_{fc}	**37**	Very high	Cold	Low	V_b
18	Middle	Very cold	High	V_{fc}	**38**	Very high	Cold	High	V_{fc}
19	Middle	Middle	Low	V_b	**39**	Very high	Hot	Low	V_{fc}
20	Middle	Middle	High	V_{fc}	**40**	Very high	Hot	High	V_{fc}

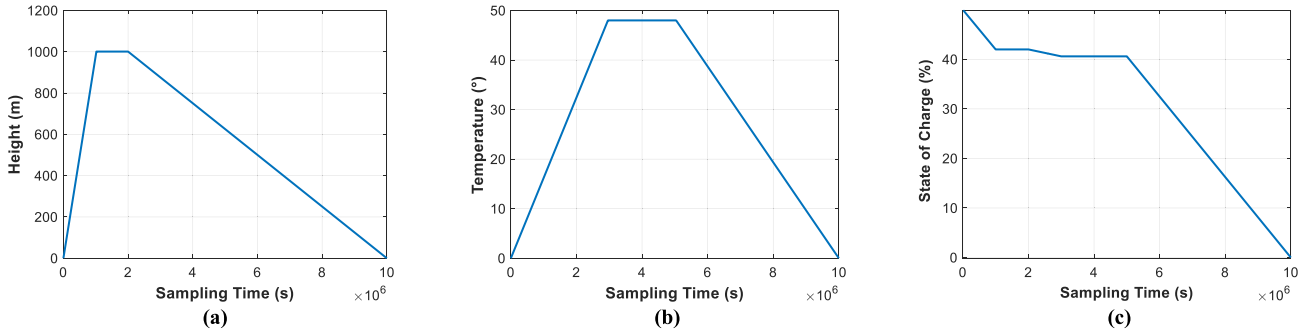

FIGURE 4. Case 1 input variable.

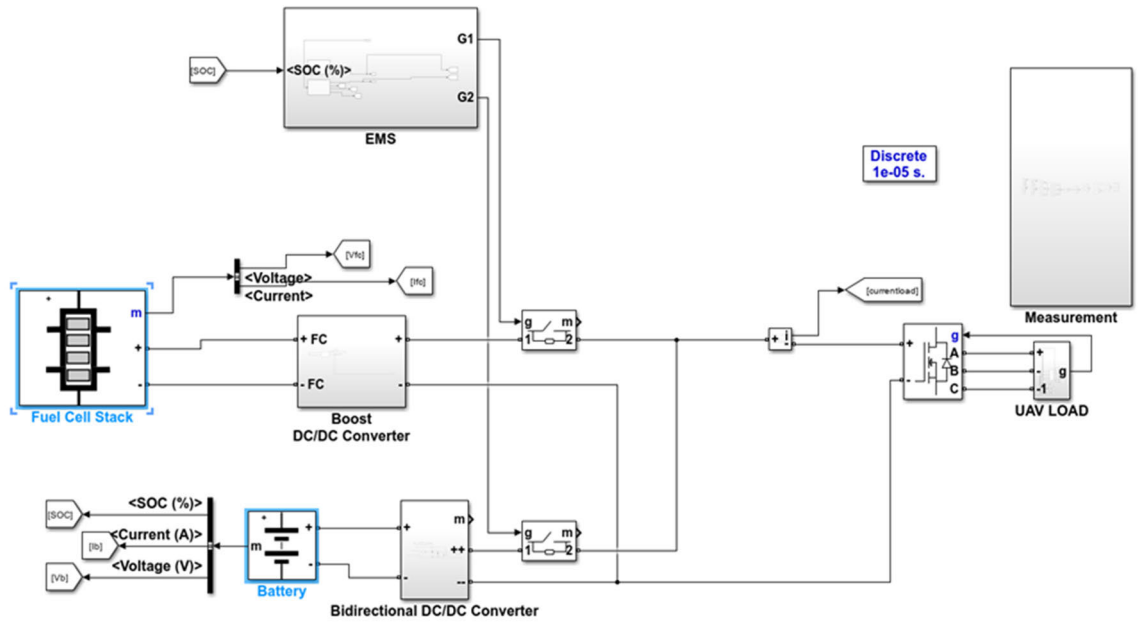

FIGURE 5. Hybrid UAV system with rule based EMS.

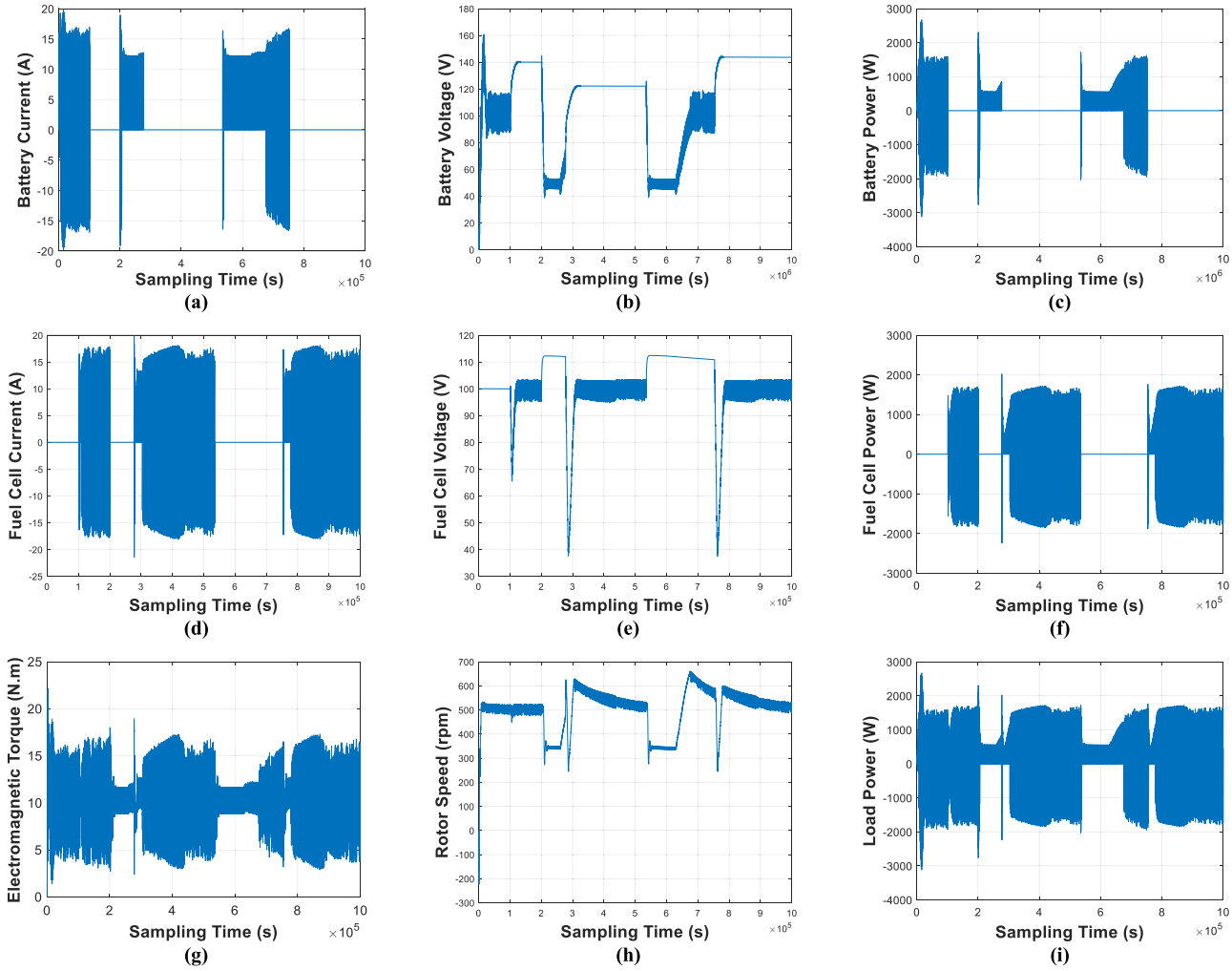

FIGURE 6. Simulation results of case 1.

is required to be constant at 100 V. But it takes time to become permanent. When it is not activated, it exceeds 100 V.

Then, it can be seen that this Figure 6-i is the sum of the power change graphs (Figure 6-c, Figure 6-f) of the battery and FC.

Change of electromagnetic torque is given in Figure 6-g and UAV rotor speed change graph is given in Figure 6-h. While the rotor speed is tried to be kept at 500 rpm, it varies depending on the availability of the sources and tries to reach 500 rpm.

B. CASE 2 (CONVENTIONAL FUZZY LOGIC EMS)

Fuzzy logic control is used to determine optimum power distribution and increase efficiency. The fuzzy logic controller uses a set of if-then statements known as rules to tie controller output to inputs. Adjectives that describe the areas of the input variables are referred to in the if section of the rules. A given input value's degree of belonging to these regions is indicated by the membership function's degree. The output variable's value is expressed in the if section of the rules. The membership degree of each part of each rule is averaged and weighted based on their membership degree in order to determine the controller's output [68].

The variables given as input to the system taken into account in the system created as a result of 40 rules are h, T and SoC, as in Case 1. The graphics of the variables given as input are as in Figure 7.

Then, in order to determine the weight status of these input values, input membership functions (IMF) are created as follows. Then, output membership functions are determined depending on whether the FC and battery are active. According to these determined functions, 40 rules are created shown in Table 5. The same rules and conditions are used for Case 3. Membership Functions of the inputs and output are seen in Figure 8.

Figure 9 shows the system created for the conventional Fuzzy and Fuzzy Type-II methods that will be examined in Case 3.

Simulation results of current, voltage and power curves of the battery and fuel cell, electromagnetic torque, rotor speed

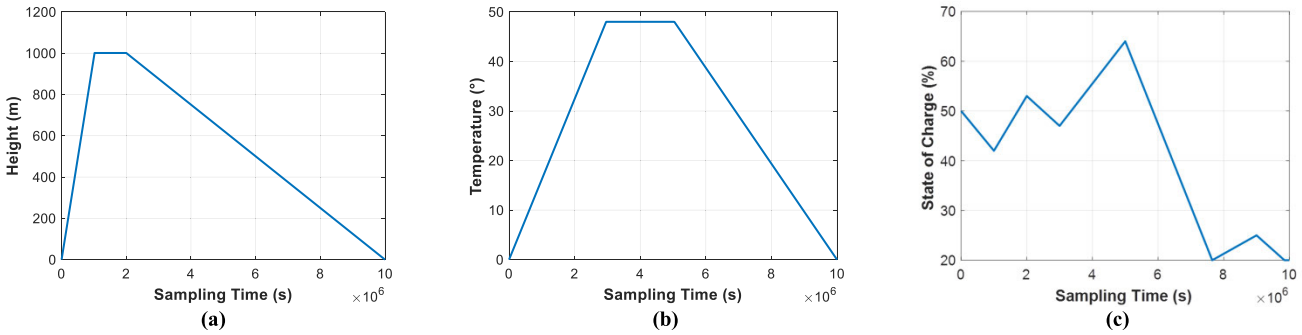

FIGURE 7. Input variables of case 2.

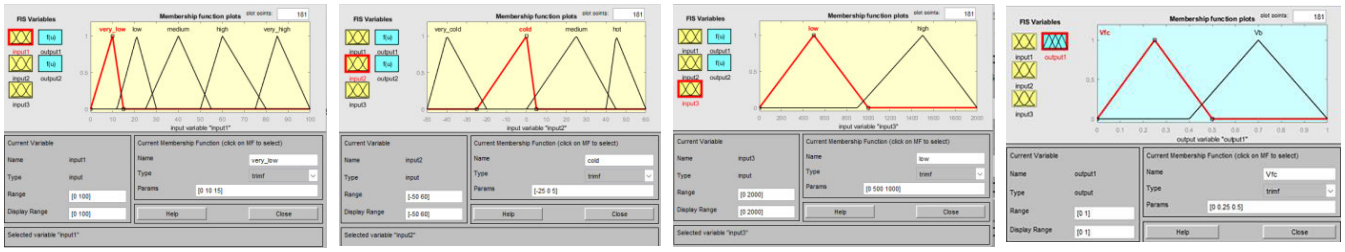

(a) IMF of SoC **(b)** IMF of Temperature **(c)** IMF of Height **(d)** Output Membership Functions

FIGURE 8. Membership functions of inputs and output.

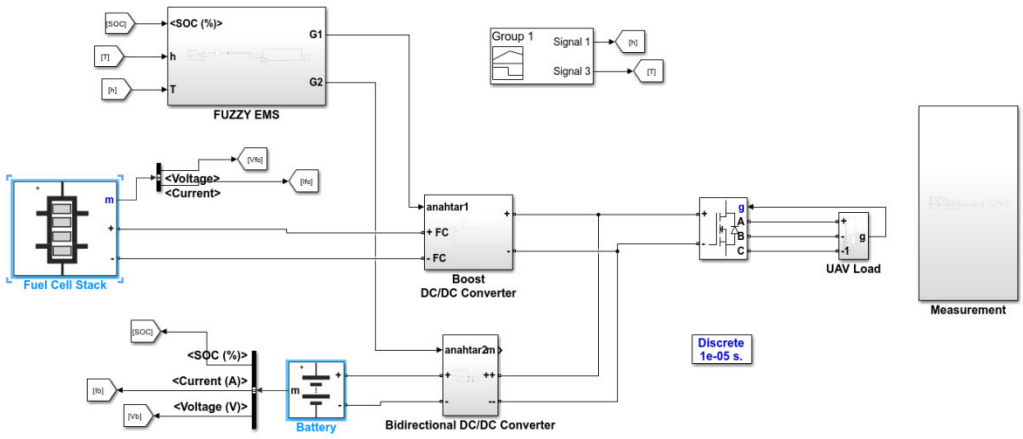

FIGURE 9. Hybrid UAV system with fuzzy logic controller for case 2 and case 3.

and load power are given in Figure 10 for Case 2 as a result of the rules.

Negative current values in Figure 10-a indicate that the battery is charged. This shows that the UAV increases its efficiency by increasing its range. Figure 10-d shows the current change graph of the FC. The fuel cell current is actually the converter output current.

As seen in Figure 10-b, in order to reach steady state, it only exceeds the nominal value at the first moment and reaches its peak value. However, in Rule-Based EMS, instantaneous peak values are recorded every time it is activated. Thus, time losses are reduced. In Figure 10-e, it only exceeds the nominal value at the first moment and reaches its peak value in order to reach steady state. However, in Rule-Based EMS,

When the change in electromagnetic torque and rotor speed in Figure 10-g and Figure 10-h is observed, it decreases compared to the oscillations in Case 1.This shows that the system is getting better.

C. CASE 3 (TYPE-II FUZZY LOGIC EMS)

Type-II fuzzy logic system emerged as a generalization of the conventional fuzzy system. Type-II fuzzy

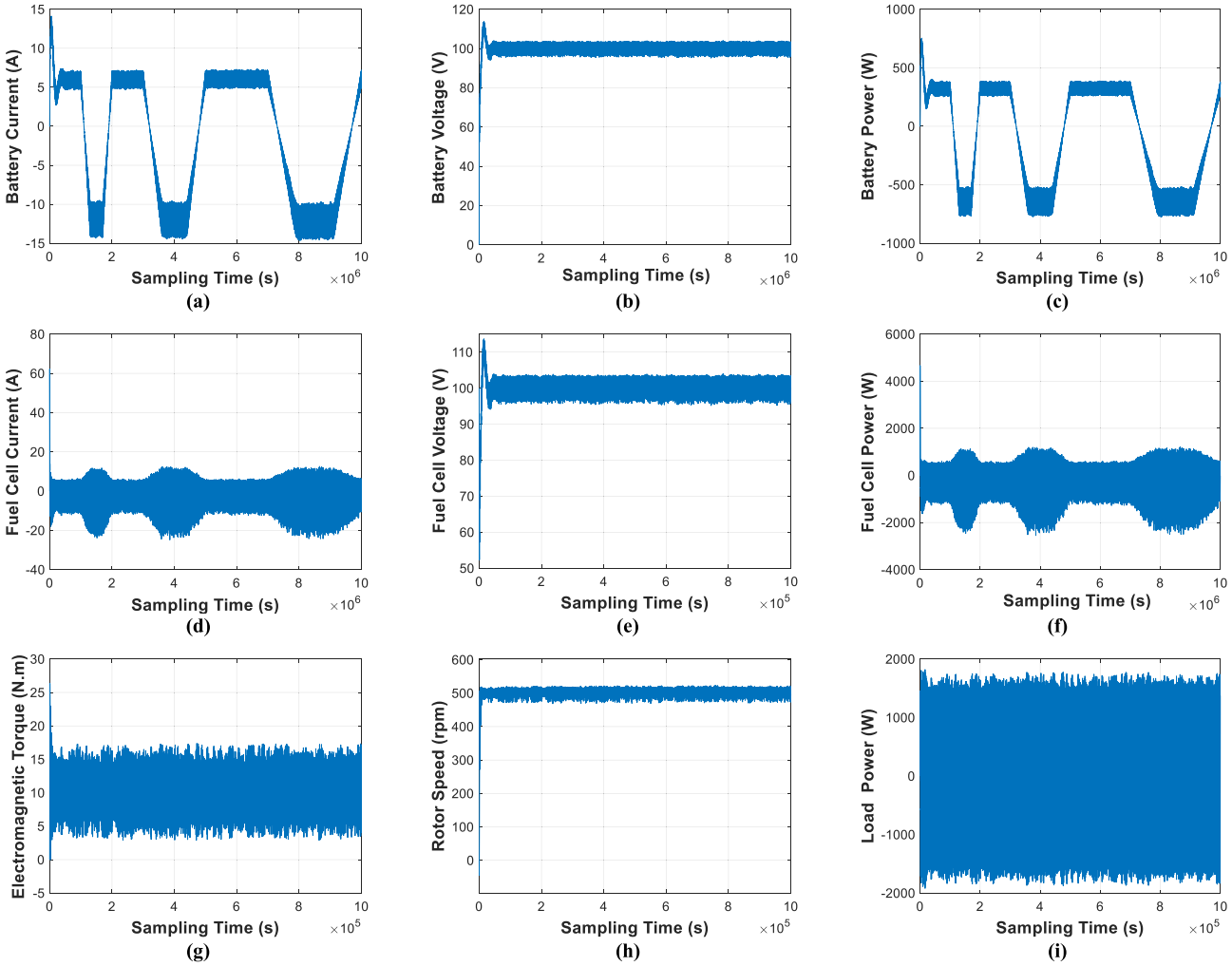

FIGURE 10. Simulation results of case 2.

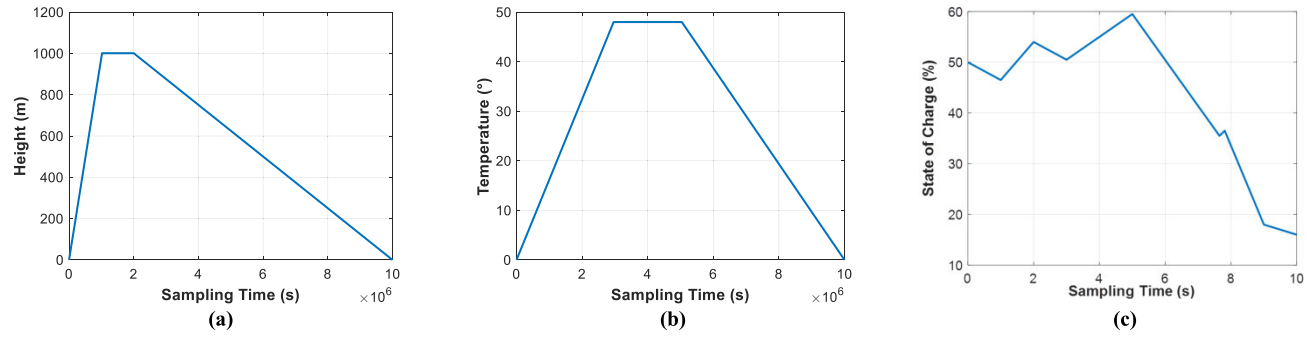

FIGURE 11. Input variables of case 3.

systems have started to be used in aviation and space applications [58].

Type-II fuzzy logic is more flexible in defining membership functions. While membership functions in classical fuzzy logic are usually defined with fixed parameters in a certain mathematical form (e.g. triangular or trapezoidal), in Type-II fuzzy logic these functions are defined with variable parameters. In this way, the system adapts to environmental variables in a more realistic and dynamic way.

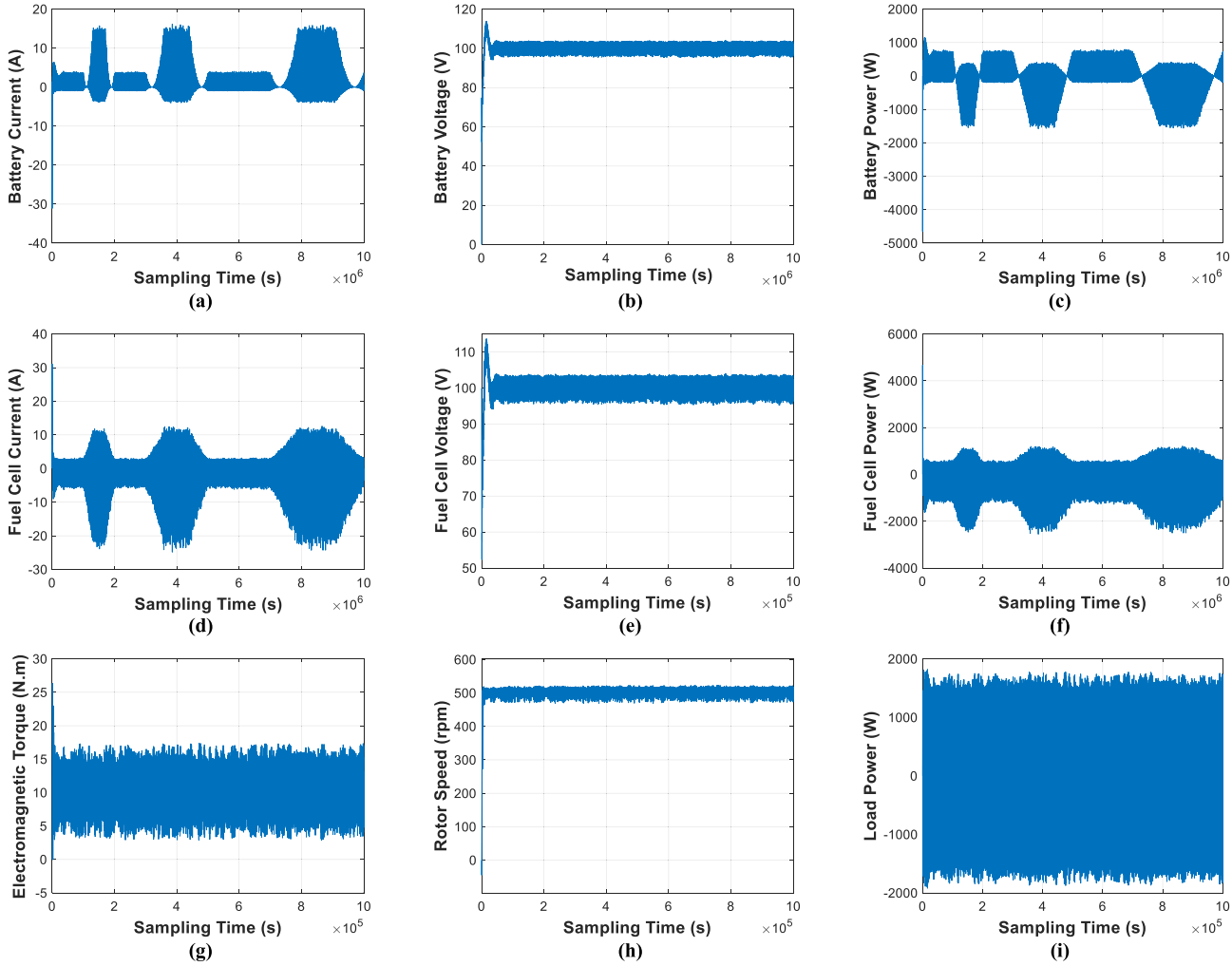

FIGURE 12. Simulation results of case 3.

The rule base is important in Type-II fuzzy logic systems. As in classical logic systems, the rule base consists of rules that determine certain input states and the outputs corresponding to these states. However, in Type-II fuzzy logic, the rules are designed to take into account the uncertainties and variability in the membership functions. In this way, the system can cope with environmental uncertainties and make correct decisions [69], [70].

The variables given as input to the system considered in the created system are h, T and SoC, as in the previous cases. The graphs of the variables given as input are as in Figure 11.

Simulation results of current, voltage and power curves of the battery and fuel cell, electromagnetic torque, rotor speed and load power are given in Figure 12 for Case 3 as a result of the rules.

As seen in the current graphs in Figure 12-a and Figure 12-d, the sharpness of the value transitions has softened in Case 3 compared to Case 2, and the amount of current drawn from the sources has increased further. The current given in Figure 12-d is actually the converter current at the fuel cell output. It can be seen that the sum of Figure 12-c and Figure 12-f exceeds the total of Figure 12-i. This explains the charging of the battery. Figure 12-g shows the electromagnetic torque and Figure 12-h shows the rotor change. The change in electromagnetic torque and rotor speed has smoother transitions than other cases.

V. CONCLUSION

In this paper, three different EMS are compared in order to control the source in the hybrid UAV system and increase the range of the UAV. Rule based on/off thermostat EMS are examined as Case 1, conventional fuzzy logic EMS as Case 2, and Type-II fuzzy logic EMS as Case 3. Some important points obtained as simulation results are listed below;

- The current drawn from the battery and FC in Case 1 varies more than Cases 2 and 3. This will cause the lifespan of the resources to decrease. Case 2 is

more advantageous than Case 3 in terms of current drawn from the sources. However, since it has a complex structure, the decision-making time increases. Since the decision-making phase is longer, the current drawn from the sources increases. This will cause the lifespan of the resources to decrease.

- Due to the DC/DC converter used, the output voltages of the battery and FC are expected to be 100 V. In Case 1, it is seen in the voltage graph of the battery and FC that the voltages rise above or remain below 100 V for a certain period of time, depending on whether they are active. This is valid only at the first moment of Cases 2 and 3. In case 1, every time it drops below or rises above 100 V, there is a loss of time to reach 100 V. From this perspective, Cases 2 and 3 are more advantageous.
- As can be seen in the power change graphs of the FC and the battery, when both graphs are added in Case 1, it is seen that the power change graph of the UAV coincides. However, in Case 1, the disadvantage is that when the sources are activated, more power is drawn from the sources than the desired power. This will cause the life of the resources to be short. Additionally, this situation causes undesirable sudden increases and decreases in the UAV power curve. Considering that the battery power change values in Case 1 are not negative, in Case 2, there is no increase or decrease in the power curves of the battery and FC except for the continuous switching process. Additionally, negative values in the battery power curve indicate increases in the SoC change graph as the SoC value of the battery increases. In case 3, it is seen that the negative power values of the battery increase. This explains the fact that the battery is being charged more and the battery SoC status is changing. However, due to its complex structure, this process takes a long time due to the difficulty of calculation.

As a result, Rule based on/off thermostat EMS should be preferred in applications where resources are required to be used separately. Conventional fuzzy logic EMS and Type-II fuzzy logic EMS should be preferred in cases where there is no sudden change in the current and voltage of the sources, the battery is charged, and the range of the UAV is desired to be increased. When evaluated in general, despite the advantages of Type-II fuzzy logic EMS, Conventional fuzzy logic EMS seems more appropriate in order to eliminate the loss of time that will occur due to complex decision making.

ACKNOWLEDGMENT

This study has been produced from Merve Nur Kaya's master's thesis.

REFERENCES

[1] M. Ayar and T. H. Karakoc, "Decision mechanism between fuel cell types: A case study for small aircraft," *Int. J. Hydrogen Energy*, vol. 48, no. 60, pp. 23156–23167, Jul. 2023, doi: 10.1016/j.ijhydene.2022.12.020.

[2] U. Kaya, Z. U. Bayrak, and E. Oksuztepe, "Fuel cell/battery hybrid powered unmanned aerial vehicle with permanent magnet synchronous motor," *Int. J. Sustain. Aviation*, vol. 3, no. 2, pp. 130–150, 2017, doi: 10.1504/ijsa.2017.086216.

[3] R. Luca, M. Whiteley, T. Neville, P. R. Shearing, and D. J. L. Brett, "Comparative study of energy management systems for a hybrid fuel cell electric vehicle—A novel mutative fuzzy logic controller to prolong fuel cell lifetime," *Int. J. Hydrogen Energy*, vol. 47, no. 57, pp. 24042–24058, Jul. 2022, doi: 10.1016/j.ijhydene.2022.05.192.

[4] A. Ursua, L. M. Gandia, and P. Sanchis, "Hydrogen production from water electrolysis: Current status and future trends," *Proc. IEEE*, vol. 100, no. 2, pp. 410–426, Feb. 2012, doi: 10.1109/JPROC.2011.2156750.

[5] A. B. Stambouli, "Fuel cells: The expectations for an environmental-friendly and sustainable source of energy," *Renew. Sustain. Energy Rev.*, vol. 15, no. 9, pp. 4507–4520, Dec. 2011, doi: 10.1016/j.rser.2011.07.100.

[6] A. Ajanovic and R. Haas, "Prospects and impediments for hydrogen and fuel cell vehicles in the transport sector," *Int. J. Hydrogen Energy*, vol. 46, no. 16, pp. 10049–10058, Mar. 2021, doi: 10.1016/j.ijhydene.2020.03.122.

[7] P. Hoenicke, D. Ghosh, A. Muhandes, S. Bhattacharya, C. Bauer, J. Kallo, and C. Willich, "Power management control and delivery module for a hybrid electric aircraft using fuel cell and battery," *Energy Convers. Manage.*, vol. 244, Sep. 2021, Art. no. 114445, doi: 10.1016/j.enconman.2021.114445.

[8] B. Wang, D. Zhao, W. Li, Z. Wang, Y. Huang, Y. You, and S. Becker, "Current technologies and challenges of applying fuel cell hybrid propulsion systems in unmanned aerial vehicles," *Prog. Aerosp. Sci.*, vol. 116, Jul. 2020, Art. no. 100620, doi: 10.1016/j.paerosci.2020.100620.

[9] A. R. Miller, J. Peters, B. E. Smith, and O. A. Velev, "Analysis of fuel cell hybrid locomotives," *J. Power Sources*, vol. 157, no. 2, pp. 855–861, Jul. 2006, doi: 10.1016/j.jpowsour.2005.12.051.

[10] O. B. Inal and C. Deniz, "Assessment of fuel cell types for ships: Based on multi-criteria decision analysis," *J. Cleaner Prod.*, vol. 265, Aug. 2020, Art. no. 121734, doi: 10.1016/j.jclepro.2020.121734.

[11] A. A. Lokhande, V. Rathore, R. Patel, R. Dudhate, and K. Kulkarni, "Hydrogen fuel cell: Parametric analysis of their stockpiling and different types," *Mater. Today, Proc.*, vol. 72, pp. 1236–1239, Jan. 2023, doi: 10.1016/j.matpr.2022.09.289.

[12] R. Xiong, J. Cao, and Q. Yu, "Reinforcement learning-based real-time power management for hybrid energy storage system in the plug-in hybrid electric vehicle," *Appl. Energy*, vol. 211, pp. 538–548, Feb. 2018, doi: 10.1016/j.apenergy.2017.11.072.

[13] M. N. Kaya and Z. Ural Bayrak, "Detailed analysis of Li-ion batteries for use in unmanned aerial vehicles," *Turkish J. Sci. Technol.*, vol. 19, no. 1, pp. 295–304, Mar. 2024, doi: 10.55525/tjst.1437348.

[14] G. Lopez Lopez, R. Schacht Rodriguez, V. M. Alvarado, J. F. Gomez-Aguilar, J. E. Mota, and C. Sandoval, "Hybrid PEMFC-supercapacitor system: Modeling and energy management in energetic macroscopic representation," *Appl. Energy*, vol. 205, pp. 1478–1494, Nov. 2017, doi: 10.1016/j.apenergy.2017.08.063.

[15] O. Veneri, C. Capasso, and S. Patalano, "Experimental study on the performance of a ZEBRA battery based propulsion system for urban commercial vehicles," *Appl. Energy*, vol. 185, pp. 2005–2018, Jan. 2017, doi: 10.1016/j.apenergy.2016.01.124.

[16] M. Zandi, A. Payman, J.-P. Martin, S. Pierfederici, B. Davat, and F. Meibody-Tabar, "Energy management of a fuel cell/supercapacitor/battery power source for electric vehicular applications," *IEEE Trans. Veh. Technol.*, vol. 60, no. 2, pp. 433–443, Feb. 2011, doi: 10.1109/TVT.2010.2091433.

[17] T. Graf, R. Fonk, S. Paessler, C. Bauer, J. Kallo, and C. Willich, "Low pressure influence on a direct fuel cell battery hybrid system for aviation," *Int. J. Hydrogen Energy*, vol. 50, pp. 672–681, Jan. 2024, doi: 10.1016/j.ijhydene.2023.09.003.

[18] Z. Fu, L. Zhu, F. Tao, P. Si, and L. Sun, "Optimization based energy management strategy for fuel cell/battery/ultracapacitor hybrid vehicle considering fuel economy and fuel cell lifespan," *Int. J. Hydrogen Energy*, vol. 45, no. 15, pp. 8875–8886, Mar. 2020, doi: 10.1016/j.ijhydene.2020.01.017.

[19] J. Y. Yong, V. K. Ramachandaramurthy, K. M. Tan, and N. Mithulananthan, "A review on the state-of-the-art technologies of electric vehicle, its impacts and prospects," *Renew. Sustain. Energy Rev.*, vol. 49, pp. 365–385, Sep. 2015, doi: 10.1016/j.rser.2015.04.130.

[20] A. Yilanci, I. Dincer, and H. K. Ozturk, "A review on solar-hydrogen/fuel cell hybrid energy systems for stationary applications," *Prog. Energy Combustion Sci.*, vol. 35, no. 3, pp. 231–244, Jun. 2009, doi: 10.1016/j.pecs.2008.07.004.

[21] S. F. Tie and C. W. Tan, "A review of energy sources and energy management system in electric vehicles," *Renew. Sustain. Energy Rev.*, vol. 20, pp. 82–102, Apr. 2013, doi: 10.1016/j.rser.2012.11.077.

[22] I. M. Abdelqawee, A. W. Emam, M. S. ElBages, and M. A. Ebrahim, "An improved energy management strategy for fuel cell/battery/supercapacitor system using a novel hybrid jellyfish/particle swarm/BAT optimizers," *J. Energy Storage*, vol. 57, Jan. 2023, Art. no. 106276, doi: 10.1016/j.est.2022.106276.

[23] A. S. Mohammed, S. M. Atnaw, A. O. Salau, and J. N. Eneh, "Review of optimal sizing and power management strategies for fuel cell/battery/super capacitor hybrid electric vehicles," *Energy Rep.*, vol. 9, pp. 2213–2228, Dec. 2023, doi: 10.1016/j.egyr.2023.01.042.

[24] T. Yigit and H. Celik, "Speed controlling of the PEM fuel cell powered BLDC motor with FOPI optimized by MSA," *Int. J. Hydrogen Energy*, vol. 45, no. 60, pp. 35097–35107, Dec. 2020, doi: 10.1016/j.ijhydene.2020.04.091.

[25] A. Altinors, F. Yol, and O. Yaman, "A sound based method for fault detection with statistical feature extraction in UAV motors," *Appl. Acoust.*, vol. 183, Dec. 2021, Art. no. 108325, doi: 10.1016/j.apacoust.2021.108325.

[26] O. Yaman, "An automated faults classification method based on binary pattern and neighborhood component analysis using induction motor," *Measurement*, vol. 168, Jan. 2021, Art. no. 108323, doi: 10.1016/j.measurement.2020.108323.

[27] H. Lu, F. Tao, Z. Fu, and H. Sun, "Battery-degradation-involved energy management strategy based on deep reinforcement learning for fuel cell/battery/ultracapacitor hybrid electric vehicle," *Electric Power Syst. Res.*, vol. 220, Jul. 2023, Art. no. 109235, doi: 10.1016/j.epsr.2023.109235.

[28] G. Sefkat and M. A. Özel, "Experimental and numerical study of energy and thermal management system for a hydrogen fuel cell-battery hybrid electric vehicle," *Energy*, vol. 238, Jan. 2022, Art. no. 121794, doi: 10.1016/j.energy.2021.121794.

[29] G. Zhang, H. Li, C. Xiao, and K. Jermsittiparsert, "Optimal size selection for fuel cell and battery in a hybrid power system of the intercity locomotives," *J. Cleaner Prod.*, vol. 317, Oct. 2021, Art. no. 128498, doi: 10.1016/j.jclepro.2021.128498.

[30] X. Xiu, S. Ma, J. Yu, S. Wang, J. Qin, and H. Huang, "Performance analysis and demonstration of fuel cell/battery hybrid system for unmanned undersea vehicles," *J. Power Sources*, vol. 575, Aug. 2023, Art. no. 233151, doi: 10.1016/j.jpowsour.2023.233151.

[31] F. Tao, H. Gong, Z. Fu, Z. Guo, Q. Chen, and S. Song, "Terrain information-involved power allocation optimization for fuel cell/battery/ultracapacitor hybrid electric vehicles via an improved deep reinforcement learning," *Eng. Appl. Artif. Intell.*, vol. 125, Oct. 2023, Art. no. 106685, doi: 10.1016/j.engappai.2023.106685.

[32] Y. Shen, P. Cui, X. Wang, X. Han, and Y.-X. Wang, "Variable structure battery-based fuel cell hybrid power system and its incremental fuzzy logic energy management strategy," *Int. J. Hydrogen Energy*, vol. 45, no. 21, pp. 12130–12142, Apr. 2020, doi: 10.1016/j.ijhydene.2020.02.083.

[33] H. Fallah Ghavidel and S. M. Mousavi-G, "Modeling analysis, control, and type-2 fuzzy energy management strategy of hybrid fuel cell-battery-supercapacitor systems," *J. Energy Storage*, vol. 51, Jul. 2022, Art. no. 104456, doi: 10.1016/j.est.2022.104456.

[34] H. Liu, X. Xing, W. Shang, and T. Li, "NSGA-II optimized multiobjective predictive energy management for fuel cell/battery/supercapacitor hybrid construction vehicles," *Int. J. Electrochemical Sci.*, vol. 16, no. 4, p. 21046, Apr. 2021, doi: 10.20964/2021.04.24.

[35] R. Rodriguez, J. P. F. Trovão, and J. Solano, "Fuzzy logic-model predictive control energy management strategy for a dual-mode locomotive," *Energy Convers. Manage.*, vol. 253, Feb. 2022, Art. no. 115111, doi: 10.1016/j.enconman.2021.115111.

[36] Z. Cheng, H. Liu, P. Yu, L. Zhu, T. Sun, and Y. Yao, "Energy management for fuel cell/battery hybrid unmanned aerial vehicle," *Int. J. Electrochemical Sci.*, vol. 16, no. 9, Sep. 2021, Art. no. 210919, doi: 10.20964/2021.09.13.

[37] H.-B. Yuan, W.-J. Zou, S. Jung, and Y.-B. Kim, "Optimized rule-based energy management for a polymer electrolyte membrane fuel cell/battery hybrid power system using a genetic algorithm," *Int. J. Hydrogen Energy*, vol. 47, no. 12, pp. 7932–7948, Feb. 2022, doi: 10.1016/j.ijhydene.2021.12.121.

[38] C. Xiao, B. Wang, C. Wang, and Y. Yan, "Design of a novel fully-active PEMFC-lithium battery hybrid power system based on two automatic ON/OFF switches for unmanned aerial vehicle applications," *Energy Convers. Manage.*, vol. 292, Sep. 2023, Art. no. 117417, doi: 10.1016/j.enconman.2023.117417.

[39] A. Townsend, I. N. Jiya, C. Martinson, D. Bessarabov, and R. Gouws, "A comprehensive review of energy sources for unmanned aerial vehicles, their shortfalls and opportunities for improvements," *Heliyon*, vol. 6, no. 11, Nov. 2020, Art. no. e05285, doi: 10.1016/j.heliyon.2020.e05285.

[40] E. Oksuztepe, Z. U. Bayrak, and U. Kaya, "Effect of flight level to maximum power utilization for PEMFC/supercapacitor hybrid uav with switched reluctance motor thruster," *Int. J. Hydrogen Energy*, vol. 48, no. 29, pp. 11003–11016, Apr. 2023, doi: 10.1016/j.ijhydene.2022.12.160.

[41] T. Jamal, G. M. Shafiullah, F. Dawood, A. Kaur, M. T. Arif, R. Pugazhendhi, R. M. Elavarasan, and S. F. Ahmed, "Fuelling the future: An in-depth review of recent trends, challenges and opportunities of hydrogen fuel cell for a sustainable hydrogen economy," *Energy Rep.*, vol. 10, pp. 2103–2127, Nov. 2023, doi: 10.1016/j.egyr.2023.09.011.

[42] Z. Zhang, Y.-X. Wang, H. He, and F. Sun, "A short- and long-term prognostic associating with remaining useful life estimation for proton exchange membrane fuel cell," *Appl. Energy*, vol. 304, Dec. 2021, Art. no. 117841, doi: 10.1016/j.apenergy.2021.117841.

[43] Z. U. Bayrak and M. T. Gencoglu, "Simulation and experimental study of a hybrid system for different loads," in *Proc. Int. Conf. Renew. Energy Res. Appl. (ICRERA)*, Milwaukee, WI, USA, Oct. 2014, pp. 451–456, doi: 10.1109/ICRERA.2014.7016426.

[44] W. Dai, H. Wang, X.-Z. Yuan, J. J. Martin, D. Yang, J. Qiao, and J. Ma, "A review on water balance in the membrane electrode assembly of proton exchange membrane fuel cells," *Int. J. Hydrogen Energy*, vol. 34, no. 23, pp. 9461–9478, Dec. 2009, doi: 10.1016/j.ijhydene.2009.09.017.

[45] G. Zhu, Y. Tian, M. Liu, Y. Zhao, W. Wang, M. Wang, Q. Li, and K. Xie, "Comprehensive competitiveness assessment of ammonia-hydrogen fuel cell electric vehicles and their competitive routes," *Energy*, vol. 285, Dec. 2023, Art. no. 129471, doi: 10.1016/j.energy.2023.129471.

[46] Y. Wang, X. Yang, Z. Sun, and Z. Chen, "A systematic review of system modeling and control strategy of proton exchange membrane fuel cell," *Energy Rev.*, vol. 3, no. 1, Mar. 2024, Art. no. 100054, doi: 10.1016/j.enrev.2023.100054.

[47] M. S. Çetin, B. Karakaya, and M. Gençoğlu, "Modelling of lithium ion batteries for electric vehicles," *Firat Univ. J. Eng. Sci.*, vol. 33, no. 2, pp. 755–763, 2021, doi: 10.35234/fumbd.953296.

[48] N. Lapeña-Rey, J. Mosquera, E. Bataller, F. Ortí, C. Dudfield, and A. Orsillo, "Environmentally friendly power sources for aerospace applications," *J. Power Sources*, vol. 181, no. 2, pp. 353–362, Jul. 2008, doi: 10.1016/j.jpowsour.2007.11.045.

[49] O. Yaman, F. Yol, and A. Altinors, "A fault detection method based on embedded feature extraction and SVM classification for UAV motors," *Microprocess. Microsyst.*, vol. 94, Oct. 2022, Art. no. 104683, doi: 10.1016/j.micpro.2022.104683.

[50] X. Li, M. Li, M. Habibi, N. Najaafi, and H. Safarpour, "Optimization of hybrid energy management system based on high-energy solid-state lithium batteries and reversible fuel cells," *Energy*, vol. 283, Nov. 2023, Art. no. 128454, doi: 10.1016/j.energy.2023.128454.

[51] J. P. Torreglosa, F. Jurado, P. García, and L. M. Fernández, "Application of cascade and fuzzy logic based control in a model of a fuel-cell hybrid tramway," *Eng. Appl. Artif. Intell.*, vol. 24, no. 1, pp. 1–11, Feb. 2011, doi: 10.1016/j.engappai.2010.08.009.

[52] M. Sparano, M. Sorrentino, G. Troiano, G. Cerino, G. Piscopo, M. Basaglia, and C. Pianese, "The future technological potential of hydrogen fuel cell systems for aviation and preliminary co-design of a hybrid regional aircraft powertrain through a mathematical tool," *Energy Convers. Manage.*, vol. 281, Apr. 2023, Art. no. 116822, doi: 10.1016/j.enconman.2023.116822.

[53] C. Vidal, O. Gross, R. Gu, P. Kollmeyer, and A. Emadi, "XEV Li-ion battery low-temperature effects—Review," *IEEE Trans. Veh. Technol.*, vol. 68, no. 5, pp. 4560–4572, May 2019, doi: 10.1109/TVT.2019.2906487.

[54] W. Tian, L. Liu, X. Zhang, J. Shao, and J. Ge, "A coordinated optimization method of energy management and trajectory optimization for hybrid electric UAVs with PV/Fuel Cell/Battery," *Int. J. Hydrogen Energy*, vol. 50, pp. 1110–1121, Jan. 2024, doi: 10.1016/j.ijhydene.2023.11.030.
[55] Y. Xie, A. Savvaris, and A. Tsourdos, "Fuzzy logic based equivalent consumption optimization of a hybrid electric propulsion system for unmanned aerial vehicles," *Aerosp. Sci. Technol.*, vol. 85, pp. 13–23, Feb. 2019, doi: 10.1016/j.ast.2018.12.001.
[56] J. M. Mendel and R. I. B. John, "Type-2 fuzzy sets made simple," *IEEE Trans. Fuzzy Syst.*, vol. 10, no. 2, pp. 117–127, Apr. 2002.
[57] T. J. Ross, *Fuzzy Logic With Engineering Applications*. Hoboken, NJ, USA: Wiley, 2024.
[58] A. Loskutov, A. Dar'enkov, I. Lipuzhin, A. Shalukho, R. Bedretdinov, V. Vanyaev, and A. Shakhov, "Energy management system for hybrid PEMFC-battery power source for stationary consumers," *Int. J. Hydrogen Energy*, vol. 55, pp. 1109–1121, Feb. 2024, doi: 10.1016/j.ijhydene.2023.11.275.
[59] I. Kocaarslan, S. Kart, Y. Altun, and N. Genc, "Lyapunov based PI controller for PEM fuel cell based boost converter," *Int. J. Renew. Energy Res.*, vol. 10, no. 1, pp. 275–280, 2020.
[60] M. A. Celik, N. Genc, and H. Uzmus, "Experimental verification of interleaved hybrid DC/DC boost converter," *J. Power Electron.*, vol. 22, no. 10, pp. 1665–1675, Oct. 2022, doi: 10.1007/s43236-022-00471-5.
[61] S. Kart, F. Demir, I. Kocaarslan, and N. Genc, "Increasing PEM fuel cell performance via fuzzy-logic controlled cascaded DC–DC boost converter," *Int. J. Hydrogen Energy*, vol. 54, pp. 84–95, Feb. 2024, doi: 10.1016/j.ijhydene.2023.05.130.
[62] (Feb. 1, 2024). *Documentation of 6 kW 45 Vdc Fuel Cell Stack in Mathworks*. [Online]. Available: https://ch.mathworks.com/help/sps/ug/6-kw-45-vdc-fuel-cell-stack.html
[63] M. Jain, M. Daniele, and P. K. Jain, "A bidirectional DC–DC converter topology for low power application," *IEEE Trans. Power Electron.*, vol. 15, no. 4, pp. 595–606, Jul. 2000, doi: 10.1109/63.849029.
[64] J. M. Andújar, F. Segura, and M. J. Vasallo, "A suitable model plant for control of the set fuel cell-DC/DC converter," *Renew. Energy*, vol. 33, no. 4, pp. 813–826, Apr. 2008, doi: 10.1016/j.renene.2007.04.013.
[65] (Feb. 1, 2024). *Documentation of Universal Bridge in Mathworks*. [Online]. Available: https://ch.mathworks.com/help/sps/powersys/ref/universalbridge.html
[66] J. Larminie and A. Dicks, *Fuel Cell Systems Explained*. Hoboken, NJ, USA: Wiley, 2003.
[67] R. Comert, U. Avdan, and E. Senkal, "Unmanned aerial vehicles usage areas and future expectations," in *Proc. Remote Sens. Geographic Inf. Syst. Symp.*, Zonguldak, Turkey, Oct. 2012, pp. 16–19.
[68] K.-S. Jeong, W.-Y. Lee, and C.-S. Kim, "Energy management strategies of a fuel cell/battery hybrid system using fuzzy logics," *J. Power Sources*, vol. 145, no. 2, pp. 319–326, Aug. 2005, doi: 10.1016/j.jpowsour.2005.01.076.
[69] Q. Liang and J. M. Mendel, "Interval type-2 fuzzy logic systems: Theory and design," *IEEE Trans. Fuzzy Syst.*, vol. 8, no. 5, pp. 535–550, Oct. 2000, doi: 10.1109/91.873577.
[70] H. A. Hagras, "A hierarchical type-2 fuzzy logic control architecture for autonomous mobile robots," *IEEE Trans. Fuzzy Syst.*, vol. 12, no. 4, pp. 524–539, Aug. 2004, doi: 10.1109/tfuzz.2004.832538.

ZEHRA URAL BAYRAK received the degree in electrical and electronics engineering from Firat University, Elâzığ, Türkiye, in 2004, the M.D. degree in electrical and electronics engineering from Dicle University, in 2007, and the Ph.D. degree in electrical and electronics engineering from Firat University, in 2014. She is currently working as an Assistant Professor with the Department of Avionics, Firat University. Her current research interests include design and analysis of renewable energy sources (fuel cells, solar cells, etc.) and hybrid power systems in unmanned aerial vehicles.

MERVE NUR KAYA was born in Elâzığ, Türkiye, in 1998. She received the degree in electrical and electronics engineering from Firat University, Elâzığ, in 2021, where she is currently pursuing the master's degree with the Department of Avionics.